Accepted Manuscript

Synthesis, anticancer, and docking studies of salicyl-hydrazone analogues: A novel series of small potent tropomyosin receptor kinase A inhibitors

Mohammad Sayed Alam, Sang-Un Choi, Dong-Ung Lee

PII: S0968-0896(16)31112-9
DOI: http://dx.doi.org/10.1016/j.bmc.2016.11.005
Reference: BMC 13371

To appear in: *Bioorganic & Medicinal Chemistry*

Received Date: 11 September 2016
Revised Date: 1 November 2016
Accepted Date: 2 November 2016

Please cite this article as: Sayed Alam, M., Choi, S-U., Lee, D-U., Synthesis, anticancer, and docking studies of salicyl-hydrazone analogues: A novel series of small potent tropomyosin receptor kinase A inhibitors, *Bioorganic & Medicinal Chemistry* (2016), doi: http://dx.doi.org/10.1016/j.bmc.2016.11.005

Synthesis, anticancer, and docking studies of salicyl-hydrazone analogues: a novel series of small potent tropomyosin receptor kinase A inhibitors

Mohammad Sayed Alam [a,b], Sang-Un Choi [c], Dong-Ung Lee [a,*]

[a] *Division of Bioscience, Dongguk University, Gyeongju 780-714, Republic of Korea*

[b] *Department of Chemistry, Jagannath University, Dhaka 1100, Bangladesh*

[c] *Center for Drug Discovery Technology, Korea Research Institute of Chemical Technology, 141 Gajeongro, Daejeon 34114, Republic of Korea*

*Corresponding author. Tel. +82 54 742 2224; fax: +82 54 742 9833.

E-mail address: dulee@dongguk.ac.kr (D.U. Lee)

ABSTRACT

A series of novel salicyl-hydrazone analogues were synthesized and evaluated for their *in vitro* cytotoxic activities in five human cancer cell lines, namely, lung cancer (A549), ovarian cancer (SK-OV-3), skin cancer (SK-MEL-2), colon cancer (HCT15) and pancreatic cancer (MIA-PaCa-2) cells, and for their *in vitro* tropomyosin receptor kinase A (TrkA) inhibitory activities. Each of the compounds showed significant cytotoxicity against all cancer cells. Compound **3i** was found to be most potent against all cancer cell lines with IC_{50} values of 2.46 (A549), 0.87 (SK-OV-3), 1.43 (SK-MEL-2), 0.89 (HCT15), and 0.48 μM (MIA-PaCa-2), followed by compound **3l**. Cytotoxicity of **3i** was similar to that of doxorubicin (0.87 μM) against HCT15 cells. Compounds **3i** and **3l** also showed highest TrkA inhibitory activities with IC_{50} values of 0.231 and 0.380 μM, respectively. A SAR study of the series revealed that compounds with hydroxyl groups showed better cytotoxicity and TrkA inhibitory potency (in the following order 2,4-OH> 2,3,4-OH>3,4-OH> 4-OH) than compounds possessing electron donating or withdrawing groups on the benzylidenephenyl ring. Docking studies of compounds **3i** and **3l** conducted on the crystal structure of TrkA receptor (a promising target for anticancer agents) showed both had a high docking score and similar order of experimental TrkA inhibitory activities. The formation of several hydrogen bonds involving N and O containing moieties contributed most significantly to ligand binding and stabilization at the active site of the receptor. In addition, ligand-receptor complexes were further stabilized by π-cation, π-anion, amide-π stacked, and van der Waal's interactions. Conformational analyses showed ligand molecules adopted similar conformations at the receptor active site during interactions, but that the low energy optimized conformations of compounds **3i** and **3l** differed.

Keywords: Salicyl-hydrazones; Cytotoxicity; TrkA inhibitor; Docking study; Conformational analysis

1. Introduction

Tropomyosin receptor kinases (Trks) are a small subfamily of the largest family of protein kinases, and are central regulators of signal transduction and controllers of various complex cellular processes.[1,2] Trk receptor plays a crucial role in the development and maintenance of the central and peripheral nervous system by activating neurotrophins (a family of high affinity growth factors). The Trk subfamily includes three highly homologues isoforms,[2] namely, TrkA, TrkB and TrkC (also known as NTRK1, NTRK2 and NTRK3, respectively), which are activated by nerve growth factor (NGF),[3] brain-derived neurotrophic factor (BDNF), by and neurotrophin-4/5 (NT-4/5)[4] or neurotrophin-3 (NT-3),[5] respectively. TrkA protein is highly expressed in sympathetic, trigeminal, and dorsal root ganglia and in cholinergic neurons of the basal forebrain and striatum.[6,7] TrkB is expressed in the central and peripheral nervous systems, whereas TrkC is widely found in mammalian neural tissues.[8,9] Non-neuronal tissues, such as, salivary glands, stomach, intestines, pancreas, bone marrow, adrenal glands, prostate, ovary, uterus, skeletal muscle and skin also produce Trk receptors in man. All three Trk receptors contain three segments, specifically, an extracellular ligand binding domain, a transmembrane domain, and an intracellular kinase domain. The binding of specific ligands activates receptor oligomerization, induces phosphorylation of specific tyrosine residues in the receptor kinase domain, and activates downstream signal transduction pathways, including survival, proliferation, and differentiation pathways in normal and neoplastic neuronal cells.[10,11] In addition, experimental evidence accumulated over the last two decades shows Trks are also involved in malignant transformation, chemotaxis, metastasis, and survival signaling in human cancers, including,

prostate,[12] pancreatic,[13] colon,[14] papillary thyroid,[15] and lung cancer,[16] breast carcinoma,[17] acute myelogenous leukemia,[18] and neuroblastoma.[19] Therefore, Trks are viewed as a promising target for development of new drugs for the treatment of different human cancers.

A literature survey revealed much effort has been devoted over the past few decades to the development of TrkA inhibitors as novel anticancer and antinociceptive drugs. These endeavors have identified various TrkA inhibitors possessing pyrimidine, 4-amino-pyrazolopyrimidine amide, pyridoquinoxaline, pyrrolidinyl urea, pyrrolopyrimidine, and alkyline-pyrimidine amide, and isothiazole scaffold as a major structural feature,[20,21] The majority of TrkA inhibitors were identified by the high-throughput screening of small molecule libraries, by using structural tailoring of known inhibitors, or by *in silico* screening of chemical libraries of small molecules using docking simulations. Figure 1 shows some TrkA inhibitors reported in the literature with a common amide (-NHCO-) functional group and N and O donor moieties.

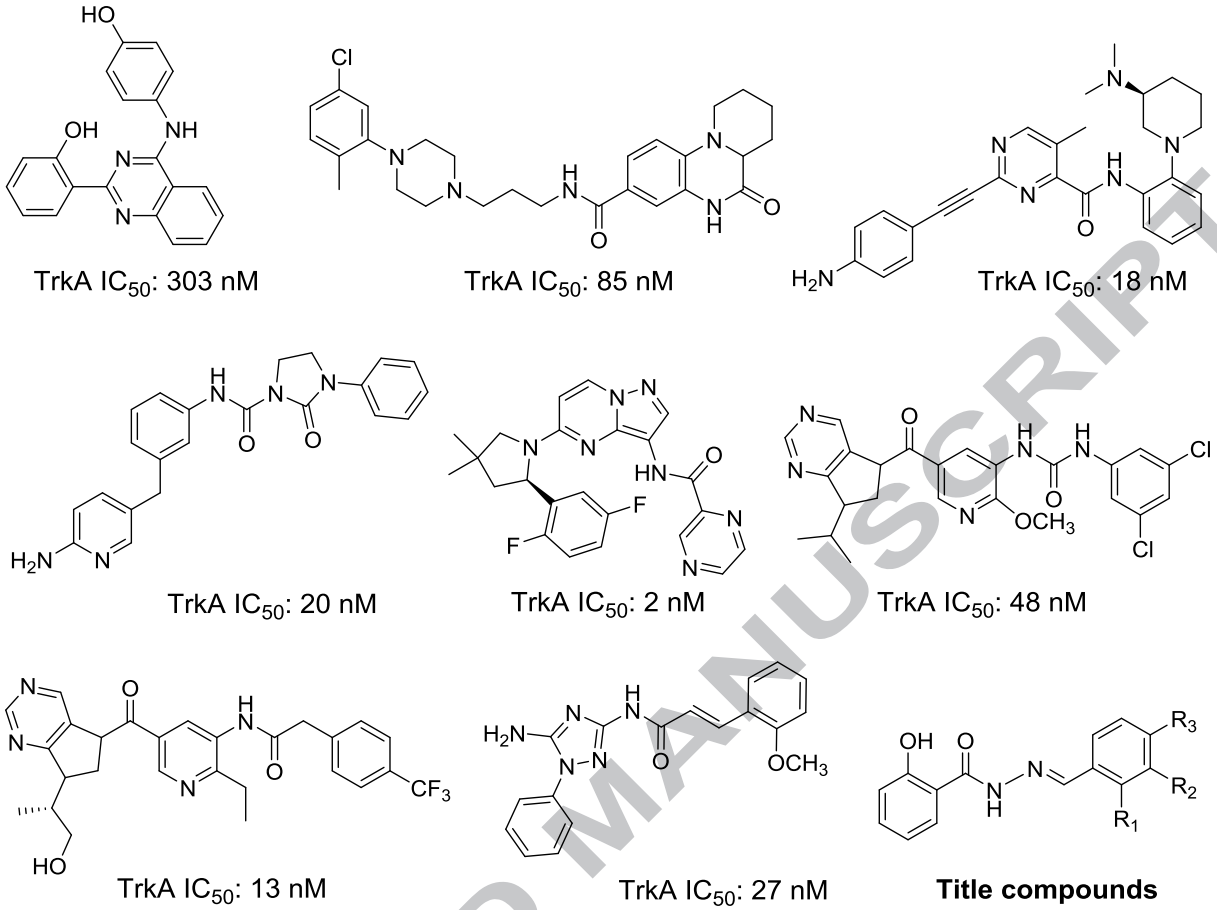

Figure 1. Chemical structures of several reported TrkA inhibitors and their reported IC_{50} values.

Small bioactive molecules are attracting growing interests in the therapeutic chemistry field. Salicylic acid (2-hydroxybenzoic acid) derivatives are a class of small molecules with surprisingly complex biological properties.[22] Chemically, salicylic acid possesses an aromatic ring with a hydroxyl group or a functionalized hydroxyl group. This scaffold is found in a variety of natural and synthetic bioactive compounds used as pharmaceuticals and agrochemicals. Salicylic acid and its functional analogues have attracted continued interest in medicinal chemistry field during the last several decades due to their wide ranging biological

activities. For example, acetylsalicylic acid (aspirin), salicylamide, methyl salicylate, diflunisal, 4-amino salicylic acid, salicylic acid azides (mesalazine, olsalizine, and balsazide), furo-salicylic acid, salicin, saligenin, salicyl-hydrazones, -pyrazoles, and -oxadiazoles are used as analgesic, antipyretic, antiinflammatory, antibacterial, antifungal, antiulcerogenic, antiplatelet, antitubercular**,** antioxidant, and sedative-hypnotic agents.[23-31] Furthermore, Gasco et al.[32] suggested *o*-acyl salicylic acid derivatives could be use as anticancer agents, particular for the treatment of colon, bladder, and prostate cancer.

During our continuing studies on the identification of novel biologically active molecules, we synthesized a series of salicyl-hydrazone analogues possessing an amide (-NHCO-) functional group and N and O donor moieties and evaluated their *in vitro* anticancer activities against five human cancer cell lines, namely, lung cancer (A549), ovarian cancer (SK-OV-3), skin cancer (SK-MEL-2), colon cancer (HCT15) and pancreatic cancer (MIA-PaCa-2) cells. The TrkA inhibitory activities of the synthesized compounds were evaluated using *in vitro* enzyme assay to investigate the mechanism responsible for their anticancer effects. Finally, docking simulation was performed using the X-ray crystallographic structure of TrkA receptor to investigate binding at its active site. To the best of our knowledge, this report is the first example to describe the TrkA inhibitory effects of salicylic acid derivatives.

2. Results and discussion

2.1. Synthesis and characterization

A series of new salicyl-hydrazone analogues (**3a-l**) were synthesized using a convenient and straightforward two-step reaction process under mild condition in ethanolic solution (Scheme 1).

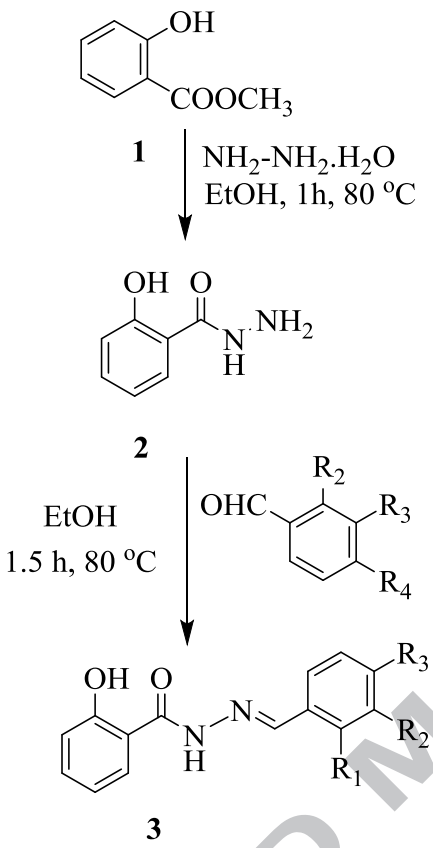

	R1	R2	R3
3a =	**H**	**H**	**H**
3b =	**H**	**H**	**Cl**
3c =	**H**	**H**	**NO_2**
3d =	**NO_2**	**H**	**H**
3e =	**H**	**H**	**NMe_2**
3f =	**H**	**H**	**CH_3**
3g =	**H**	**H**	**OH**
3h =	**H**	**H**	**OCH_3**
3i =	**OH**	**H**	**OH**
3j =	**OCH_3**	**H**	**OCH_3**
3k =	**H**	**OH**	**OH**
3l =	**OH**	**OH**	**OH**

Scheme 1. The synthesis of salicyl-hydrazone analogues.

Overall isolated yields of the synthesized compounds were excellent (68.37- 87.5 %). Structural characterizations were performed by FT-IR, ^{1}H NMR, mass spectrometry, and elemental analysis. The FT-IR spectra of compounds **3a-l** showed characteristic amide >C=O and –NH- group stretch absorption bands around 1628–1665 and 3112-3268 cm^{-1}, respectively. Phenolic –OH stretch absorption bands were observed at around 3200-3561 cm^{-1}. In the ^{1}H NMR spectra of compounds **3a-l**, azomethine (–CH=N-) and amide (-NHCO-) protons showed characteristic singlets at 8.30-8.87 and 11.60-12.17 ppm, respectively, equivalent to one proton

each. The *N*,*N*′-dimethyl (-N(CH_3)$_2$) and aromatic methyl (Ar-CH_3) protons of **3e** and **3f** appeared as singlets at 2.97 and 2.35 ppm equivalent to six and three protons, respectively, while the methoxy protons of compounds **3h** and **3j** were observed at around 3.83-3.89 ppm as a singlet equivalent to three proton each. Other aromatic protons expected peaks that depended on substitution pattern. In their EI-mass spectra, compounds **3a-l** produced molecular ion peaks with intensities of 7-93%.

2.2. Cytotoxic activities

The *in vitro* cytotoxic activities of salicyl-hydrazone analogues (**3a-l**) were screened against five human carcinoma cell lines, that is, lung cancer (A549), ovarian cancer (SK-OV-3), skin cancer (SK-MEL-2), colon cancer (HCT15) and pancreatic cancer (MIA-PaCa-2) cells using the sulforhodamine-B (SRB) method.[33] To evaluate cytotoxic activities, inhibitions of net cell proliferation were measured after incubating cells with test samples for 48 h. Inhibitions are expressed as percentages of non-treated controls. The cytotoxicities of compounds (**3a-l**) are presented in Table 1, and their activities were compared with doxorubicin (a standard anticancer agent), which was used as a positive control. All 12 compounds studies showed cytotoxic activities against the four cancer cell lines. Among them, compound **3i** exhibited greatest cytotoxic effect against all cancer cell lines, followed in decreasing order by compounds **3l**, **3g** **3a,** and **3k**. Compound **3i** had a cytotoxic potency similar to doxorubicin against HCT15 cancer cells (IC_{50} 0.89 μM *vs* 0.872 μM), but lower potency against A549 (2.46 μM), SK-OV-3 (IC_{50} 0.87 μM) SK-MEL-2 (1.43 μM) and MIA-PaCa-2 (0.48 μM) cancer cells (corresponding IC_{50} values for doxorubicin were 0.021, 0.74, 0.001 and 0.049 μM, respectively).

Table 1

In vitro cytotoxicity data of the salicyl-hydrazone analogues (**3a-l**)

Comp.	IC_{50} values/μM[a]				
	A549[b]	SK-OV-3[c]	SK-MEL-2[d]	HCT15[e]	MIA-PaCa-2[f]
3a	2.78	5.94	9.77	21.31	2.46
3b	22.19	9.83	14.28	20.85	7.19
3c	8.72	8.80	9.34	22.67	6.73
3d	23.15	19.61	19.40	34.59	14.04
3e	21.48	18.52	19.33	38.39	20.67
3f	6.74	9.81	13.05	26.91	4.45
3g	2.86	9.10	5.46	8.60	1.18
3h	12.92	14.36	15.17	28.06	8.64
3i	2.46	0.87	1.43	0.89	0.48
3j	31.27	14.52	19.61	25.74	11.32
3k	3.15	9.14	8.86	10.03	4.74
3l	7.16	1.96	1.84	3.71	2.21
Doxorubicin	0.021	0.074	0.001	0.872	0.049

[a]IC_{50} values were obtained using dose response curves by nonlinear regression using a curve fitting program (OriginPro 7.5). [b]human lung cancer, [c]human ovarian cancer, [d]human skin cancer, [e]human colon cancer and [f]human pancreatic cancer.

The structure activity relationship study revealed that the natures and positions of substituents on the benzylidenephenyl ring have significant effects on cytotoxic activities. Compound **3i** with hydroxyl groups (OH) at *ortho*- and *para*- positions in benzylidenephenyl ring showed greater cytotoxicity against all five cell lines than **3a**, which has a non-substituted benzylidenephenyl ring. Whereas, compound **3k** with hydroxyl groups at *meta*- and *para*-

position in its benzylidenephenyl ring had less cytotoxic effect on all cell lines than compound **3i**. However, compound **3k** showed similar activity against A549 (IC_{50} 3.15 μM) and SK-MEL-2 (IC_{50} 8.86 μM) cells, but less and more activity against SK-OV-3 (IC_{50} 9.14 μM), HCT15 (IC_{50} 10.03 μM) and MIA-PaCa-2 (IC_{50} 4.74 μM) cells than **3a** (Table 1). Interestingly, the introduction of an additional hydroxyl group at the *ortho*-position in benzylidenephenyl ring of **3k** to produce **3l** resulted in a ~2-5 fold increase in activity against SK-OV-3 (IC_{50} 1.96 μM), SK-MEL-2 (IC_{50} 1.84 μM), HCT15 (IC_{50} 3.71 μM) and MIA-PaCa-2 (IC_{50} 2.21 μM) cells but reduced activity against A549 cells (IC_{50} 7.16 μM) by ~2.5 fold. Compound **3g** with one hydroxyl group at the *para*-position of the benzylidenephenyl ring exhibited ~2-3 times greater activity against SK-MEL-2 (IC_{50} 5.46 μM), HCT15 (IC_{50} 8.60 μM) and MIA-PaCa-2 (IC_{50} 1.18 μM) cells but similar activity against A549 (IC_{50} 2.86 μM), and less activity against SK-OV-3 (IC_{50} 9.10 μM), respectively, than **3a (**IC_{50} values 9.77, 21.31, 2.78 , 5.94 and 2.46 μM for SK-MEL-2, HCT15, A549, SK-OV-3 and MIA-PaCa-2, respectively**)**. Methylation of **3g** and **3i** to produce **3h** and **3j**, respectively, resulted in significant activity reductions against all cell lines**.** Introduction of an electron donating group to **3a**, namely, *N*,*N*-dimethylamino (**3e**), methyl (**3f**), or methoxy (**3h**), or an electron withdrawing group, namely, chloro (**3b**) or nitro (**3c**), at the *para*-position of benzylidenephenyl ring reduced activity against all five cell lines. The above results show the presence of a hydroxy (OH) group at the *ortho*- and *para*- positions in the benzylidenephenyl ring increased cytotoxic activity against the cell lines used in the present study. Additional cytotoxicity assays on different salicyl-hydrazone analogues are required to confirm and expand structure activity relationships.

2.3. TrkA inhibitory activity

The TrkA inhibitory activities of the salicyl-hydrazones (**3a-l**) were also examined. Results are presented in Table 2. Compound **3i**, which had greatest cytotoxic activity, also showed greatest TrkA inhibitory activity (IC_{50}: 0.231 μM) followed by compound **3l** (IC_{50}: 0.380 μM).

Table 2

TrkA kinase inhibitory activities of the salicyl-hydrazone analogues (**3a-l**)

Compound	TrkA inhibition (%)[a]	Compound	TrkA inhibition (%)[a]
3a	-	**3g**	20.62
3b	6.92	**3h**	-
3c	-	**3i**	92.38 (0.2315)[b]
3d	-	**3j**	7.61
3e	-	**3k**	92.88 (2.545)[b]
3f	3.70	**3l**	90.90 (0.380)[b]
		GW441756	>99.0 (0.003)[b]

[a]Inhibition rate at 1 μM. [b]Values in parentheses represent IC_{50} (μM). "-" : Not active at a concentration of 1 μM

Compound **3k** also showed significant TrkA inhibitory activity with an IC_{50} of 2.545 μM. The other nine compounds exhibited low or no activity at 1 μM. GW441756 (1,3-Dihydro-3-[(1-methyl-1*H*-indol-3-yl)methylene]-2*H*-pyrrolo[3,2-*b*]pyridin-2-one),[34,35] an oxindole analogue has been used as a positive control to compare the TrkA inhibitory activity of the synthesized compounds. GW441756 is well-known potent selective TrkA inhibitor which displays 100-fold greater selectivity over a range of other kinases. However, GW441756 exerted lower IC_{50} value of 3 nM compare to that of salicyl-hydrazone analogues. Interestingly, compounds with a

hydroxyl group in the benzylidenephenyl ring exhibited excellent TrkA inhibitory activities in the following order 2,4-OH> 2,3,4-OH>3,4-OH> 4-OH.

2.4. Docking studies

To predict interaction modes and affinities and provide a guide for further SAR studies, simulations were performed on the docking of compounds **3i** and **3l** into the active site of TrkA receptor. The crystal structure of TrkA receptor was obtained from the Protein Data Bank (PDB ID: 4f0i), and a summary of the docking studies is presented in Table 3.

Table 3

Docking energies and molecular interactions of salicyl-hydrazone ligands with TrkA receptor.

Entry	Binding affinity (Kcal/mol)	Energy contribution		Average conpair	H-bonding residues (distance, Å)	Other interacting residues
		vdW	H-bond			
3i	-107.506	-58.431	-49.075	23.350	His648 (2.65) Asn655 (2.63) Gly670 (2.38) Arg673(2.54)	Glu560, Leu564, Phe589, Phe646, Asp650, Gly667, Asp668, Met671, Ser672, Tyr680
3l	-103.194	-60.873	-42.321	22.905	His648 (2.35) Asn655 (2.74) Asp668 (2.76) Ser672 (2.38)	Glu560, Leu564, Phe589, Phe646, Ile666, Asp650, Gly667, Gly670, Arg673, Met671, Tyr680

The results obtained showed compounds **3i** and **3l** bind to the same active site as previously reported for TrkA inhibitors[36,37] by hydrogen bonding and hydrophobic, electrostatic, covalent, and Van der Wall's interactions. Calculated binding modes and interactions of **3i** and **3l** are shown in Figs. 2 and 3, respectively.

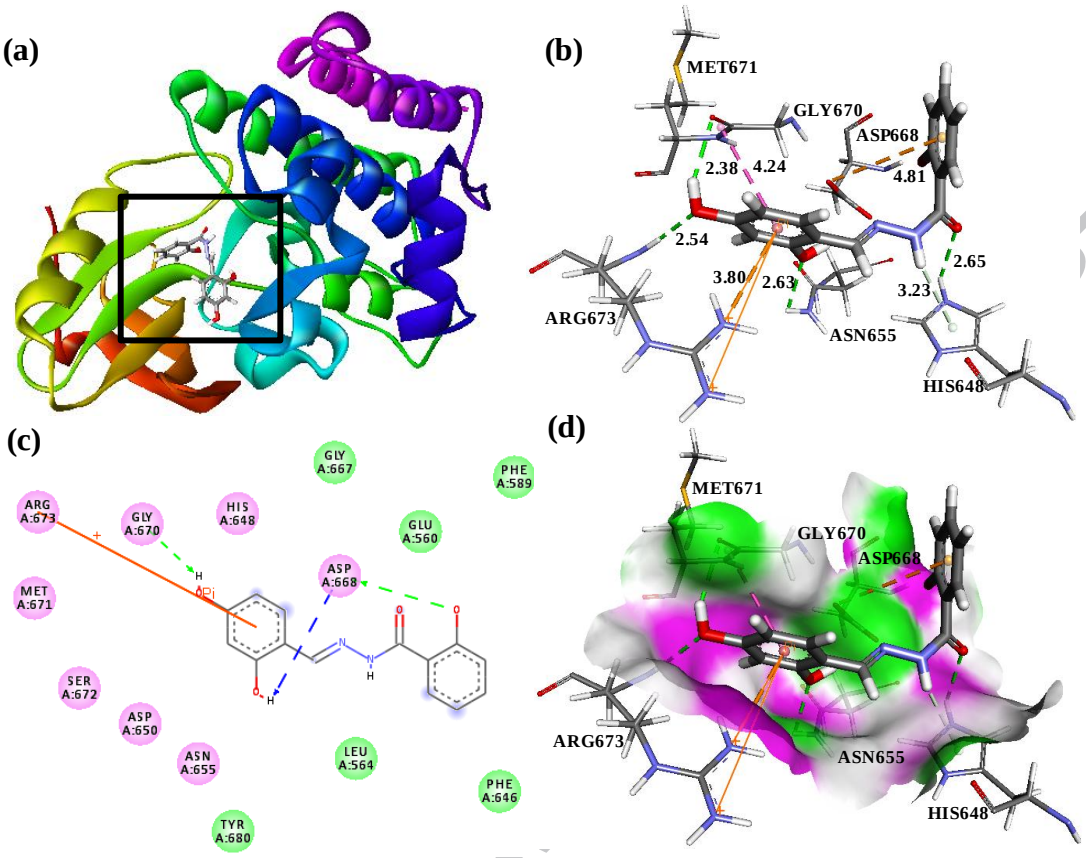

Figure 2. (a) A general view of a ligand/TrkA receptor complex. The black square shows the zone of ligand-TrkA interactions. (**b**) Binding of compound **3i** with TrkA receptor (Protein Data Bank ID: 4f0i). The *green dotted lines* represent hydrogen bonds, the *gold dotted lines* π-cation or anion interactions, the *pink dotted line* shows an amide-π stacked interaction, and the *light green dotted line* a π-donor interaction. (**c**) 2D ligand interaction diagram with TrkA receptor obtained using the Discovery Studio program; essential amino acid residues at the binding site are circled. The *purple circles* show amino acids involved in electrostatic and covalent interactions and the *green circles* show amino acids exhibiting van der Waals interactions. (**d**) Hydrogen bond interaction showing donor (pink) and acceptor surfaces (green).

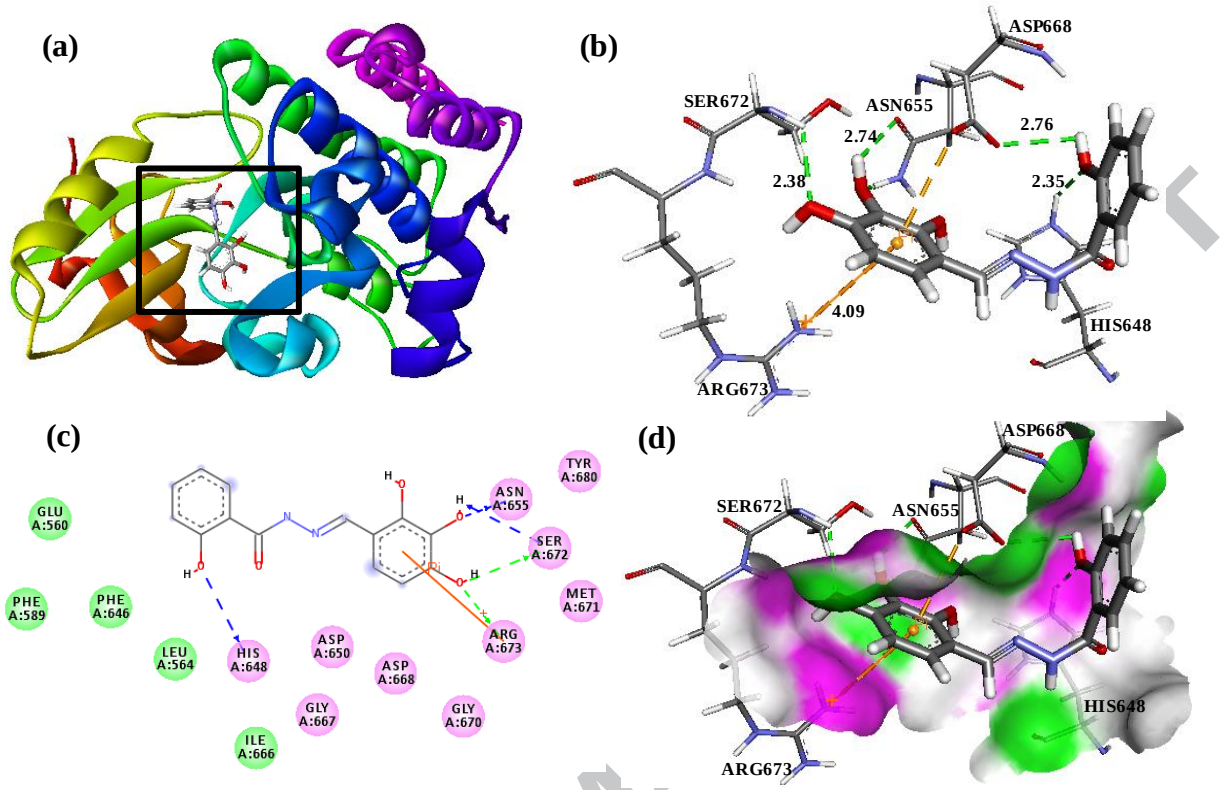

Figure 3. (a) A general view of a ligand-TrkA receptor complex. The black square shows the zone of ligand-kinase interactions. (**b**) Binding of compound **3l** with TrkA receptor (Protein Data Bank ID: 4f0i). The *green dotted lines* represents hydrogen bonds, and the *gold dotted lines* π-cation or anion interactions. (**c**) 2D ligand interaction diagram with TrkA receptor obtained using the Discovery Studio program; essential amino acid residues at the binding site are circled. The *purple circles* show amino acids involved in electrostatic and covalent interactions and the *green circles* amino acids involved in van der Waals interactions. (**d**) Hydrogen bond interaction showing donor (pink) and acceptor surfaces (green).

Both compounds interacted with the same amino acid residues with few exceptions, and both formed four hydrogen bonds, which appeared to contribute most to ligand stabilization in the binding site. Binding scores for compounds **3i**, and **3l** were calculated using iGEMDOCK software[38] and their binding affinities with TrkA receptor were found to be -107.506 and -103.194 kcalmol^{-1}, respectively, with hydrogen bond contributions of -49.075 and -42.321

kcalmol^{-1}, respectively, and van der Waal contributions of 58.431 and 60.873 kcalmol^{-1}, respectively. Specifically, **3i** forms hydrogen bonds using its carbonyl oxygen atom with His648 (H…O=C<: 2.65Å), and the *ortho*- and *para*-hydroxyl groups of its benzylidene phenyl ring bond with Asn655 (O…H–O: 2.63Å), Gly670 (H…O–H: 2.38Å), and Arg673 (O…H–O: 2.54Å) amino acid residues. On the other hand, compound **3l** hydrogen bonds using the *ortho*-hydroxyl group of its benzoyl phenyl ring with His648 (H…O–H: 2.35Å) and Asp668 (O…H–O: 2.76Å), and using the *meta*- and *para*-hydroxyl groups of its benzylidene phenyl ring with the amino acid residues of Asn655 (O…H–O: 2.74Å) and Ser672 (H…O–H: 2.38Å). Compounds **3i** and **3l** were further stabilized in the binding site by a π-cation interaction between the benzylidenephenyl ring and Arg673 and by π-anion interaction between the benzoylphenyl ring of **3i** and benzylidenephenyl ring of **3l** and Asp668. In addition to these interactions, compounds **3i** and **3l** also exhibited van der Waal's interactions with Glu560, Leu564, Phe589, Phe646 (only for **3i**), Asp650, Gly667, Met671, Ser672 (only for **3i**), and Tyr680 and Ile666 (only for **3l**). In addition, an amide-π stacked interaction was also observed between Gly670 and the benzylidenephenyl ring of **3i**. The above results suggest the additional electrostatic and van der Waal's interactions of **3i** explain its lower total binding energy and resulted in highest potency (TrkA IC_{50} 231 nm) compare to that of **3l** (TrkA IC_{50} 380 nm).

2.5. Conformational analysis

Conformational analysis was performed to better understand the bioactive conformations of the salicyl-hydrazone analogues by superimposing the lowest energy optimized and docked bioactive conformations of compounds **3i** and **3l**. A comparison of the optimized and bioactive conformations of compounds **3i** and **3l** are shown in Fig. 4. The lowest energy conformer was

obtained by calculation using the MM2 semi-empirical molecular orbital method[39] and bioactive conformer was obtained by docking simulation allowing free rotation about single bonds of ligands.

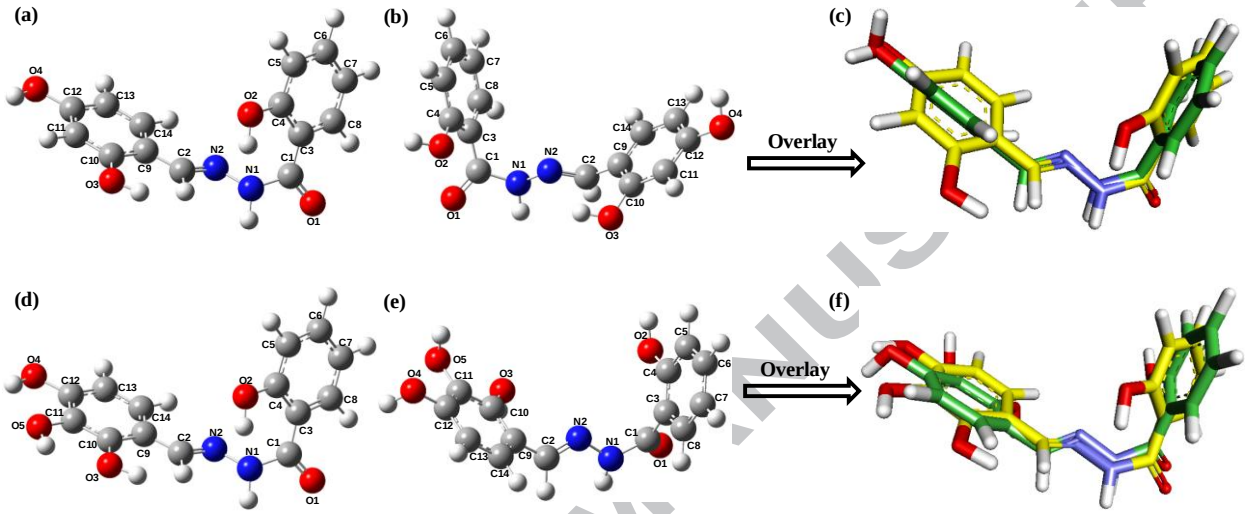

Figure 4. 3D geometries (**a** and **d**) of optimized and (**b** and **e**) of bioactive conformations of compounds **3i** and **3l**, respectively. (**c** and **f**) Show overlays of the optimized (yellow) and bioactive (green) conformations of compounds **3i** and **3l**, respectively.

Biologically active molecules can adopt several conformations of nearly equal torsion energy, which is related to torsion angles produced by rotating about single bonds to achieve interactions in receptor-active sites. As shown in Fig. 4, the bioactive conformers of compounds **3i** and **3l** obviously differed from their corresponding optimized conformers. In particular, for **3i**, torsion angles around the N2-C2-C9-C14 bond of the optimized and bioactive conformers were 0.18, and 74.12°, respectively, and torsion angles around the O1-C1-C3-C4 bond were -163.86 and 54.72°, respectively. While for **3l**, optimized and bioactive torsion angles around the N2-C2-C9-C14 bond were 0.26, and -125.08°, respectively, and torsion angles around the O1-C1-C3-C4

bond were -163.89 and 63.25°, respectively. Analysis of these conformations indicated both the benzylidene and benzoyl phenyl ring of **3l** deviated (by 125.34 and 227.14°, respectively) during docking to adopt the bioactive conformation, whereas deviations of **3i** were 73.94 and 218.58°, respectively. MM2 calculated torsion energies were -6.4865 and -10.4168 kcalmol^{-1} for **3i** and **3l**, respectively. The above results indicate the optimized conformer of **3l** is more stable, and therefore, requires more energy to adopt the bioactive conformation, and that this results in lower receptor binding affinity than that of **3i**. This observation is consistent with our docking and experimental results. It is also worth noting compounds **3i** and **3l** adopted similar bioactive conformations (Fig. 5) at the receptor binding site, though their optimized conformations were quite different.

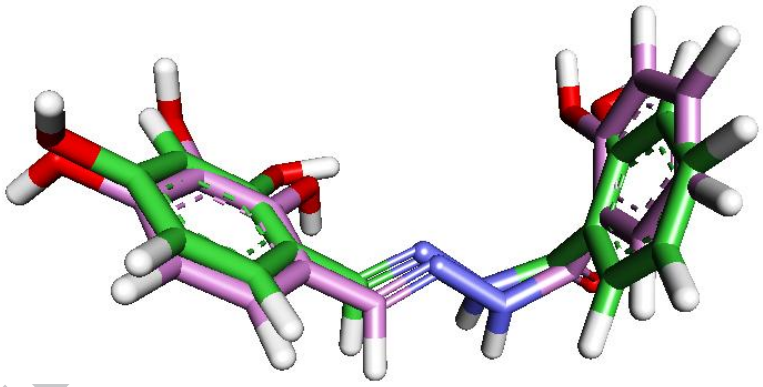

Figure 5. Superimposition of the bioactive conformations of compound **3i** (green) and **3l** (violet).

3. Conclusion

A new series of salicyl-hydrazone analogues were synthesized and evaluated for *in vitro* cytotoxic activity against five human cancer cell lines, that is, lung cancer (A549), ovarian cancer (SK-OV-3), skin cancer (SK-MEL-2), colon cancer (HCT15) and pancreatic cancer

(MIA-PaCa-2) cell lines. The *in vitro* TrkA inhibitory activities of these analogues were screened to examine their modes of action. All 12 tested compounds showed significant cytotoxicities against the four cancer cell lines. Compound **3i** showed greatest cytotoxic potency against all cancer cell lines, followed in decreasing order by compounds **3l**, **3g, 3a** and **3k**. Compound **3i**, which had hydroxyl groups at the *ortho*- and *para*-positions of its benzylidenephenyl ring exhibited a potency similar to doxorubicin against HCT15 cancer cells with an IC_{50} value of 0.89 μM, but showed lower potency against A549, SK-OV-3, SK-MEL-2 and MIA-PaCa-2 cells (IC_{50} values for **3i** were 2.46, 0.87, 1.43, 0.48 μM, and those of doxorubicin were 0.872, 0.021, 0.74, 0.001 and 0.049 μM, respectively). TrkA inhibitory assays also showed compound **3i** was most potent with an IC_{50} value of 231 nM was followed in decreasing order by **3l**, **3k** and **3g**. The structure-activity relationship study revealed that salicyl-hydrazone analogues with hydroxyl groups on the benzylidenephenyl ring showed better cytotoxic and TrkA inhibitory activities in the order 2,4-OH> 2,3,4-OH>3,4-OH> 4-OH than analogues bearing electron donating (e.g. $-N(CH_3)_2$, $-CH_3$, and $-OCH_3$) or withdrawing (e.g. $-NO_2$, and -Cl) groups on the benzylidenephenyl ring. Docking studies were performed to investigate interactions between the highest potent analogues (**3i** and **3l)** and the active site of TrkA receptor. These studies revealed that **3i** and **3l** bound in the same manner as has been reported for TrkA inhibitors with a high docking score. Conformational analysis led us to speculate that compounds **3i** and **3l** adopt similar conformations during interaction with TrkA receptor, despite quite different optimized conformations. These results provide a valuable starting point for the design and synthesis of salicyl-hydrazone analogues that inhibit TrkA as potential anticancer agents.

4. Experimental

4.1. General

Melting points of the twelve synthesized compounds were determined using a Stuart SMP3 apparatus and results were uncorrected. FT-IR spectra were obtained using a Bruker Tensor 37 spectrometer and KBr discs. NMR spectra were recorded using an AM-400 MHz (Bruker, USA) spectrometer in DMSO using TMS as the internal standard. Mass spectra were acquired using a Jeol JMS700 high-resolution mass spectrometer at the Korean Basic Science Center (Daegu, South Korea). Elemental analyses (C, H, N) were performed on a Flash EA 2000 series (Thermo Fisher) elemental analyzer.

4.2. General procedure for the preparations of salicyl-hydrazide (1) and salicyl-hydrazone analogues (3a-l).

Salicyl-hydrazide (2-hydroxybenzohydrazide) was prepared as we previously described.[40] Briefly, methyl salicylate (15.2 g, 0.1 M) was refluxed with hydrazine hydrate (12.5 g, 0.25 M) in approximately 50 mL of ethanol for 3 h. Reaction progress was monitored by TLC. Precipitated salicyl-hydrazide was filtered and recrystallized from an ethanol-water mixture. Physical data were compared with previously reported values to confirm structures.

Next, salicyl-benzohydrazone analogues (**3a-l**) were prepared as previously described.[37] Briefly, salicyl-hydrazide (**1**, 2 mM) in 30 mL ethanol was added drop-wise to 20 mL of suitably substituted benzaldehydes (**2**, 2 mM) dissolved in ethanol. Mixtures were stirred and refluxed for 1.5-3.0 h and reaction progress was monitored by TLC. After cooling reaction mixtures to ambient temperature, they were filtered to give solid crude products, which were crystallized from ethanol to provide the pure compounds.

4.2.1. (E)-*N*'-(benzylidene)-2-hydroxybenzohydrazide (3a)[27]

White crystals. Yield: 74.6%, mp 244-245 °C. IR (KBr) ν_{max}: 3242 (OH), 3185 (NH), 2934 (CH), 1630 cm^{-1} (C=O). ^{1}H NMR: (400 MHz; DMSO-d_6) δ 6.89-7.05 (2H, m, Ar-H), 7.37-7.59

(5H, m, Ar-H), 7.69-7.98 (2H, m, Ar-H), 8.43 (1H, s, CH), 11.81 (1H, s, NH). EI-MS *m/z* (%): 240 (M^+, 20), 137 (26), 121 (100), 120 (37). Anal. Calcd for $C_{14}H_{12}N_2O_2$ C 69.99; H 5.03; N 11.66%. Found C 69.42; H 5.14; N 11.31%.

4.2.2. (E)-N'-(4-chlorobenzylidene)-2-hydroxybenzohydrazide (3b)

White crystals. Yield 85.0%, mp 265-266°C. IR (KBr) ν_{max}: 3257 (OH), 3167 (NH), 2925 (CH), 1629 cm^{-1} (C=O). ^1H NMR (400 MHz; DMSO-d_6) δ 6.91-7.00 (2H, m, Ar-H), 7.40-7.56 (3H, m, Ar-H), 7.76-7.90 (3H, m, Ar-H), 8.45 (1H, s, CH), 11.92 (1H, s, NH). EI-MS *m/z* (%): 274 (M^+, 12), 154 (16), 137 (22), 121 (100), 120 (25). Anal. Calcd for $C_{14}H_{11}ClN_2O_2$ C 61.21; H 4.04; N 10.20%. Found C 61.28; H 4.23; N 10.11%.

4.2.3. (E)-N'-(4-nitrobenzylidene)-2-hydroxybenzohydrazide (3c)

Yellow crystals. Yield 68.4%, mp 105-106°C. IR (KBr) ν_{max}: 3379 (OH), 3249 (NH), 2937 (CH), 1632 cm^{-1} (C=O). ^1H NMR (400 MHz; DMSO-d_6) δ 6.99-7.02 (2H, m, Ar-H), 7.48-7.55 (1H, m, Ar-H), 7.92-8.09 (2H, m, Ar-H), 8.20-8.24 (1H, m, Ar-H), 8.36-8.50 (2H, m, Ar-H), 8.62 (1H, s, CH), 12.12 (1H, s, NH). EI-MS *m/z* (%): 285 (M^+, 12), 179 (5), 137 (13), 122 (12), 121 (100), 120 (19). Anal. Calcd for $C_{14}H_{11}N_3O_4$ C 58.95; H 3.89; N 14.73%. Found C 58.65; H 3.99; N 14.18%.

4.2.4. (E)-N'-(2-nitrobenzylidene)-2-hydroxybenzohydrazide (3d)

Yellow crystals. Yield 67.4%, mp 228-229°C IR (KBr) ν_{max}: 3294 (OH), 3212 (NH), 3064 (CH), 1634 cm^{-1} (C=O). ^1H NMR (400 MHz; DMSO-d_6) δ 6.94-7.02 (2H, m, Ar-H), 7.42-7.51 (1H, m, Ar-H), 7.64-7.89 (3H, m, Ar-H), 8.04-8.16 (2H, m, Ar-H), 8.87 (1H, s, CH), 12.17

(1H, s, NH). EI-MS *m/z* (%): 285 (M^+, 7), 179 (5), 137 (14), 122 (9), 121 (100), 120 (14), 118 (7). Anal. Calcd for $C_{14}H_{11}N_3O_4$ C 58.95; H 3.89; N 14.73%. Found C 59.00; H 4.03; N 16.05%.

4.2.5. (E)-N'-(4-dimethylaminobenzylidene)-2-hydroxybenzohydrazide (3e)

Yellow crystals. Yield 83%, mp 259-260 °C. IR (KBr) ν_{max}: 3282 (OH), 3210 (NH), 2917 (CH), 1632 cm^{-1} (C=O). ^1H NMR (400 MHz; DMSO-d_6) δ 2.97 (6H, s, $N(CH_3)_2$), 6.70-6.81 (2H, m, Ar-H), 6.90-7.01 (2H, m, Ar-H), 7.38-7.46 (1H, m, Ar-H), 7.51- 7.61 (2H, m, Ar-H), 7.85-8.94 (1H, m, Ar-H), 8.30 (1H, s, CH), 11.60 (1H, s, NH). EI-MS *m/z* (%): 283 (M^+, 93), 164 (11), 163 (100), 161 (41), 146 (75), 145 (15), 121 (56), 118 (10). Anal. Clcd for $C_{16}H_{17}N_3O_2$ C 67.83; H 6.05; N 14.83% Found C 67.60; H 6.21; N 15.97%

4.2.6. (E)-N'-(4-methylbenzylidene)-2-hydroxybenzohydrazide (3f)[41]

White crystals. Yield 86.0%, mp 246-247 °C. IR (KBr) ν_{max}: 3271 (OH), 3235 (NH), 2922 (CH), 1655 cm^{-1} (C=O). ^1H NMR (400 MHz; DMSO-d_6) δ 2.35 (3H, s, Ar-CH_3), 6.90- 7.02 (2H, m, Ar-H), 7.20- 7.46 (3H, m, Ar-H), 7.60-7.73 (2H, m, Ar-H), 7.84-7.92 (1H, m, Ar-H), 8.42 (1H, s, CH), 11.78 (1H, s, NH). EI-MS *m/z* (%): 254 (M^+, 23), 137 (39), 134 (67), 121 (100), 119 (18), 120 (39). Anal. Calcd for $C_{15}H_{14}N_2O_2$ C 70.85; H 5.55; N 11.02%. Found C 70.78; H 5.67; N 11.60%.

4.2.7. (E)-N'-(4-hydroxybenzylidene)-2-hydroxybenzohydrazide (3g)

Yellow crystals. Yield 72.6%, mp 177-178 °C. IR (KBr) ν_{max}: 3346 (OH), 3268 (NH), 2947 (CH), 1669 cm^{-1} (C=O). ^1H NMR (400 MHz; DMSO-d_6) δ 6.88-7.06 (3H, m, Ar-H), 7.45-7.66 (3H, m, Ar-H),7.74-7.92 (2H, m, Ar-H), 8.37 (1H, s, CH), 11.72 (1H, s, NH). EI-MS *m/z*

(%): 256 (M^+, 25), 137 (42), 136 (68), 121 (100), 120 (35). Anal. Calcd for $C_{14}H_{12}N_2O_3$ C 65.62; H 4.72; N 10.93%. Found C 62.62; H 5.24; N 9.12%.

4.2.8. (E)-N'-(4-methoxybenzylidene)-2-hydroxybenzohydrazide (3h)[41]

Yellow crystals. Yield 73.3%, mp 211-212 °C. IR (KBr) ν_{max}: 3263 (OH), 3158 (NH), 2954 (CH), 1654 cm^{-1} (C=O). ^1H NMR (400 MHz; DMSO-d_6) δ 3.85 (3H, s, OCH_3), 6.94-7.16 (4H, m, Ar-H), 7.42-7.51 (1H, m, Ar-H), 7.69-7.95 (3H, m, Ar-H), 8.42 (1H, s, CH), 11.77 (1H, s, NH). EI-MS *m/z* (%): 270 (M^+, 33), 268 (11), 150 (100), 149 (12), 137 (47), 134 (10), 121 (77), 120 (40). Anal. Calcd for $C_{15}H_{14}N_2O_3$ C 66.66; H 5.22; N 10.36%. Found C 66.74; H 5.36; N 10.80%.

4.2.9. (E)-N'-(2,4-dihydroxybenzylidene)-2-hydroxybenzohydrazide (3i)

Yellow crystals. Yield 87.5%, mp 155-156 °C. IR (KBr) ν_{max}: 3561 (OH), 3468(OH), 3200 (NH), 2913 (CH), 1628 cm^{-1} (C=O). ^1H NMR (400 MHz; DMSO-d_6) δ 6.29-6.41 (2H, m, Ar-H), 6.92-7.04 (2H, m, Ar-H), 7.29-7.49 (2H, m, Ar-H), 7.82-7.94 (1H, m, Ar-H), 8.55 (1H, s, CH), 11.37 (1H, s, NH). EI-MS *m/z* (%): 272 (M^+, 43), 152 (51), 138 (51), 137 (81), 121 (100), 120 (30). Anal. Calcd for $C_{14}H_{12}N_2O_4$ C 61.76; H 4.44; N 10.29%. Found C 58.57 H, 4.82 N, 9.50%.

4.2.10. (E)-N'-(2,4-dimethoxybenzylidene)-2-hydroxybenzohydrazide (3j)

Yellow crystals. Yield 74.3%, mp 155-156 °C. IR (KBr) ν_{max}: 3324 (OH), 3242 (NH), 2963 (CH), 1650 cm^{-1} (C=O). ^1H NMR (400 MHz; DMSO-d_6) δ 3.83 (3H, s, OCH_3), 3.89 (3H, s, OCH_3), 6.58-6.71 (2H, m, Ar-H), 6.89-7.01 (2H, m, Ar-H), 7.36-7.47 (1H, m, Ar-H), 7.67-7.87 (2H, m, Ar-H), 8.70 (1H, s, CH), 11.77 (1H, s, NH). EI-MS *m/z* (%): 300 (M^+, 55), 180 (26), 179

(12), 163 (81), 150 (10), 149 (90), 137 (45), 121 (100), 120 (45). Anal. Calcd for $C_{16}H_{16}N_2O_4$ C 63.99; H 5.37; N 9.33%. Found C 64.21; H 5.66; N 7.68%.

4.2.11. (E)-N'-(3,4-dihydroxybenzylidene)-2-hydroxybenzohydrazide (3k)

Brown powder. Yield 68.7%, mp 216-217 °C. IR (KBr) ν_{max}: 3330 (OH), 3112 (NH), 3061 (CH), 1645 cm^{-1} (C=O). ^{1}H NMR (400 MHz; DMSO-d_6) δ 6.81-7.02 (3H, m, Ar-H), 7.26-7.34 (2H, m, Ar-H), 7.43-7.50 (1H, m, Ar-H), 7.89-7.97 (1H, m, Ar-H), 8.30 (1H, s, CH), 11.60 (1H, s, NH). EI-MS *m/z* (%): 272 (M^+, 21), 152 (26), 138 (11), 137 (22), 121 (100), 120 (17). Anal. Calcd for $C_{14}H_{12}N_2O_4$ C 61.76; H 4.44; N 10.29%. Found C 60.99; H 4.55; N 7.72%.

4.2.12. (E)-N'-(2,3,4-trihydroxybenzylidene)-2-hydroxybenzohydrazide (3l)

White crystals. Yield 68.5%, mp 250-251°C. IR (KBr) ν_{max}: 3379 (OH), 3243 (NH), 2925 (CH), 1630 cm^{-1} (C=O). ^{1}H NMR (400 MHz; DMSO-d_6) δ 6.40-6.52 (1H, m, Ar-H), 6.82-7.03 (3H, m, Ar-H), 7.43-7.52 (1H, m, Ar-H), 7.88- 7.93 (1H, m, Ar-H), 8.53 (1H, s, CH), 11.92 (1H, s, NH). EI-MS *m/z* (%): 288 (M^+, 39), 168 (35), 153 (11), 137 (12), 121 (100), 120 (22). Anal. Calcd for $C_{14}H_{12}N_2O_5$ C 58.33; H 4.20; N 9.72%. Found C 55.27; H 4.77; N 8.04%.

4.3. Biological assay

4.3.1. Cytotoxicity assays

The cytotoxicities of the 12 test compounds on the four tumor cell lines were determined using the SRB (sulforhodamine-B) method, which is currently adopted by the NCI (National Cancer Institute, UK) for *in vitro* anti-cancer drug screening.[33] Inhibition of cell proliferation was estimated after continuous exposure to test compounds for 48 h. All samples were tested in

triplicate, and mean IC_{50} values (mg/mL) (concentration resulting in 50% inhibition of cell proliferation) were calculated.

4.3.2. Tropomyosin receptor kinase A (TrkA) inhibitory activity

Purified TrkA protein was purchased from Carna Biosciences (Kobe, Japan). Protein kinase, biotinylated substrate peptide, and TrkA inhibitors were pre-incubated for 15 min. at 25°C in 384-well plates. The phosphorylation reaction of TrkA enzyme was started by adding ATP **(**100 μM**)**, and 30 min later an anti-phosphotyrosine antibody (1 μM) labeled with europium (Eu) cryptate and 125 nM streptavidin labeled with fluorophore XL665 were added to reaction mixtures. After incubation for 1h, fluorescences were measured using an Envision multi-label reader (Perkin Elmer, Waltham, MA, USA) using an excitation wavelength of 320nm and emission wavelengths of 620 (Eu-labeled antibody) and 665nm (XL665-labeled streptavidin). Homogeneous time-resolved fluorescence resonance energy transfer (FRET) between Eu cryptate and XL665 was measured to quantify substrate peptide phosphorylation. The ratios of the fluorescence intensities ($\lambda_{620nm}/\lambda_{665nm}$) were calculated at 12 different serial dilutions (0.03~10000 nM) of the compounds tested. The % inhibition data was plotted against tested compound concentration to determine IC_{50} values, which were calculated by using the Prizm program (La Jolla, CA, USA). GW441756 (R&D System, Minneapolis, MN, USA), a well-known TrkA inhibitors, was used as a positive control.

4.4. Docking studies

The three-dimensional conformations of compounds **3i** and **3l** were constructed using standard bond lengths and angles using the ChemBio3D ultra Ver. 14 molecular modeling program (Cambridge Soft Corporation, Cambridge, MA 02140 USA), and energies were optimized using

the semi-empirical molecular orbital MM2 method[39] using 1810 (for **3i**) and 2264 (for **3l**) iterations and a minimum RMS gradient of 0.10. The crystal structure of tropomyosin receptor kinase A (TrkA)[37] was obtained from Protein Data Bank (PDB code: 4f0i) for docking studies. All bound water in the crystal structure of TrkA receptor was eliminated and polar hydrogen atoms and Kollman-united charges were added to molecules. The pdb and pdbqt files of ligands and the receptor were prepared using AutoDock 4.2 software.[42] Docking simulations were performed using the standard method implemented by AutoDock Vina in PyRx 0.8 software[43] and free rotations were allowed about single bonds during docking. Geometries of resulting complexes and their conformations were investigated using Discovery Studio 4.0 (Accelrys, San Diego, CA, USA) and GaussView 5.0 (Gaussian Inc., Wallingford, CT, USA).

Acknowledgements

This work was supported by the Research Fund of Dongguk University (2015).

References

1. Cohen, P. *Nat. Rev. Drug. Discov*. **2002**, *1* 309.
2. Patapoutian, A.; Reichardt, L. F. *Curr. Opin. Neurobiol*. **2001**, *11*, 272.
3. Cohen, S.; Levi-Montalcini, R.; Hamburger, V. *Proc. Natl. Acad. Sci. USA* **1954**, *40*, 1014.

4. Ip, N. Y.; Ibanez, C. F.; Nye, S. H.; McClain, J.; Jones, P. F.; Gies, D. R.; Belluscio, L.; Le Beau, M. M.; Espinosa, R. 3rd; Squinto, S. P. *Proc. Natl. Acad. Sci. USA* **199**2, *89*, 3060.
5. Lamballe, F.; Klein, R.; Barbacid, M. *Cell* **1991**, *66*, 967.
6. Kaplan, D. R.; Martin-Zanca, D.; Parada, L. F. *Nature* **1991**, *350*, 158.
7. Hempstead, B. L.; Martin-Zanca, D.; Kaplan, D. R.; Parada, L. F.; Chao, M. V. *Nature* **1991**, *350*, 678.
8. Klein, R.; Lamballe, F.; Bryant, S.; Barbacid, M. *Neuron* **1992**, *8*, 947.
9. Lamballe, F.; Klein, R.; Barbacid, M. *Cell* **1991**, *66*, 967.
10. Reichardt, L. F. *Philosophical Transactions of the Royal Society, B: Biol. Sci*. 2006, 361, 1545.
11. Skaper, S. D. *CNS Neurol. Disord. Drug Targets* **2008**, *7*, 46.
12. Papatsoris, A. G.; Liolotsa, D.; Deliveliotis, C. *Expert Opin. Invest. Drugs* **2007**, *16*, 303.
13. Sclabas, G. M.; Fujioka, S.; Schmidt, C.; Li, Z.; Frederick, W. A. I.; Yang, W.; Yokoi, K.; Evans, D. B.; Abbruzzese, J. L.; Hess, K. R.; Zhang, W.; Fidler, I. J.; Chiao, P. J.; *Clin. Cancer Res*. **2005**, *11*, 440.
14. Bardelli, A.; Parsons, D. W.; Silliman, N.; Ptak, J.; Szabo, S.; Saha, S.; Markowitz, S.; Willson, J. K. V.; Parmigiani, G.; Kinzler, K. W.; Vogelstein, B.; Velculescu, V. E. *Science* **2003**, *300*, 949.
15. Nakagawara, A. *Cancer Lett*. **2001**, *169*, 107.
16. Davies, H.; Hunter, C.; Smith, R.; Stephens, P.; Greenman, C.; Bignell, C.; Teague, J.; Butler, A.; Edkins, S.; Stevens, C.; Parker, A.; O'Meara, S.; Avis, T.; Barthorpe, S.; Brackenbury, L.; Buck, G. et al. *Cancer Res*. **2005**, *65*, 7591.

17. Lagadec, C.; Meignan, S.; Adriaenssens, E,; Foveau, B,; Vanhecke, E,; Romon, R.; Toillon, R.A.; Oxombre, B.; Hondermarck, H.; Le Bourhis, X. *Oncogene* **2009**, *28*, 1960.

18. Tognon, C.; Knezevich, S. R.; Huntsman, D.; Roskelley, C. D.; Melnyk, N.; Mathers, J. A.; Becker, L.; Carneiro, F.; MacPherson, N.; Horsman, D.; Poremba, C.; Sorensen, P. H. *Cancer Cell* **2002**, *2*, 367.

19. Brodeur, G. M. *Nat. Rev. Cancer Cell* **2003**, *3*, 203.

20. Wang, T.; Yu, D.; Lamb, M. L. *Expert Opin. Ther. Pat.* **2009**, *19*, 305.

21. McCarthy, C.; Walker, E. *Expert Opin. Ther. Pat.* **2014**, *24*, 731.

22. Ekinci, D.; Sentürk, M.; Küfrevioğlu, O. I. *Expert Opin. Ther. Pat.* **2011**, *21*, 1831.

23. Lisina, S. V.; Brel, A. K.; Mazanova, L. S.; Spasov, A. A. *Pharm. Chem. J.* **2008**, *42*, 574.

24. Hassan, G. S.; Soliman, G. A. *Eur. J. Med. Chem.* **2010**, *45*, 4104.

25. da Silva, M.; Souza Menezes, C. M.; Ferreira, E. I.; Leite, C.Q.F.; Sato, D. N.; Correia, C. C.; Pimenta, C. P.; Botelho, K. C. A. *Chem. Biol. Drug Des.* **2008**, *71*, 167.

26. Machado, P.; Rosa, F. A.; Rossatto, M.; da S. Sant'Anna, G.; Sauzem, P. D.; da Silva, R. M. S.; Rubin, M. A.; Ferreira, J.; Bonacorso, H. G.; Zanatta, N.; Martins, M. A. P. *ARKIVOC* **2007**, *16*, 281.

27. Pattan, S. R.; Rabara, P.; Pattan, J. S.; Bukitaga, A. A.; Wakale, V. S.; Musmade, D. S. *Ind. J. Chem.* **2009**, *48B*, 1453.

28. Shelke, V. A.; Jadhav, S. M.; Shankarwar, S. G.; Munde, A. S.; Chondhekar, T. K. *Bull. Chem. Soc. Ethiop.* **2011**, *25*, 381.

29. Chaturvedi, R.; Shah. J. Salicylic acid in plant disease resistance, in: Hayat, S.; Ahmad, A. (Eds.), Salicylic acid. A plant hormone, Springer, Dordrecht, The Netherlands, 2007, pp. 335-70.

30. Malamy, J.; Carr, J. P.; Klessig, D. F.; Raskin, I. *Science* **1990**, *250*, 1002.

31. Chowdhury, M. A.; Abdellatif, K. R. A.; Dong, Y.; Das, D.; Yu, G.; Velázquez, C. A.; Suresh, M. R.; Knaus, E. E. *Bioorg. Med. Chem. Lett*. **2009**, *19*, 6855.

32. Gasco, A.; Fruttero, R.; Lazzarato, R.; Donnola, M. Salicylic acid derivatives, U.S. Patent 0293781, 2008.

33. Skehan, P.; Streng, R.; Scudiero, D.; Monks, A.; McMahon, J.; Vistica, D.; Warren, J. T.; Bokesch, H.; Kenney, S.; Boyd, M. R. *J. Natl. Cancer Inst*. **1990**, *82*, 1107.

34. Wood, E. R.; Kuyper, L.; Petrov, K. G.; Hunter, R. N. III.; Harris, P. A.; Lackey K. *Bioorg. Med. Chem. Lett.* **2004**, *14*, 953.;

35. Montagnoli, C.; Pistilli, A.; Stabile, A.; Rende, R.; Rambotti, M.; Spreca, A.; Rende, M. *Ital. J. Anat. Embryol.* **2010**, *115*, 117.

36. Park, H.; Chi, O.; Kim, J.; Hong, S. *J. Chem. Inf. Model*. **2011**, *51*, 2986.

37. Bertrand, T.; Kothe, M.; Liu, J.; Dupuy, A.; Rak, A.; Berne, P. F.; Davis, S.; Gladysheva, T.; Valtre, C.; Crenne, J. Y.; Mathieu, M. *J. Mol. Biol*. **2012**, *423*, 439.

38. Yang, J. M.; Chen, C. C. *Proteins* **2004**, *55*, 288.

39. Allinger, N. L. *J. Am. Chem. Soc.* **1977**, *99*, 8127.

40. Liu, L.; Alam, M. S.; Lee, D. U. *Bull. Korean Chem. Soc*. **2012**, *33*, 3361.

41. Budiati1, T.; Stephanie, D. A.; Widjajakusuma, E. C. *Indonesian J. Chem*. **2012**, *12*, 163.

42. Morris, G. M.; Huey, R.; Lindstrom, W.; Sanner, M. F.; Belew, P. K.; Goodsell, D. S.; Olson, A. J. *J. Comput. Chem*. **2009**, *30*, 2785.

43. Trott, O.; Olson, A. J. *J. Comput. Chem*. **2010**, *31*, 455.

Graphical Abstract

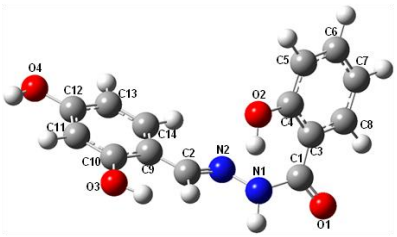

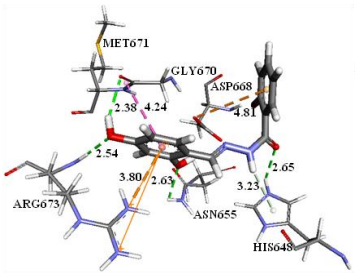

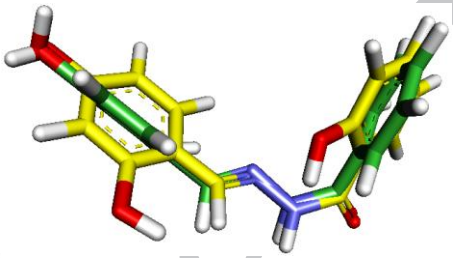

TrkA inhibitor (IC_{50}) 230 nM